

Learning Stochastic Bridges for Video Object Removal via Video-to-Video Translation

Zijie Lou ^{*1} Xiangwei Feng ^{*1} Jiaxin Wang ^{1,2} Xiaochao Qu ¹ Luoqi Liu ¹ Ting Liu ¹

Abstract

Existing video object removal methods predominantly rely on diffusion models following a noise-to-data paradigm, where generation starts from uninformative Gaussian noise. This approach discards the rich structural and contextual priors present in the original input video. Consequently, such methods often lack sufficient guidance, leading to incomplete object erasure or the synthesis of implausible content that conflicts with the scene’s physical logic. In this paper, we reformulate video object removal as a video-to-video translation task via a stochastic bridge model. Unlike noise-initialized methods, our framework establishes a direct stochastic path from the source video (with objects) to the target video (objects removed). This bridge formulation effectively leverages the input video as a strong structural prior, guiding the model to perform precise removal while ensuring that the filled regions are logically consistent with the surrounding environment. To address the trade-off where strong bridge priors hinder the removal of large objects, we propose a novel adaptive mask modulation strategy. This mechanism dynamically modulates input embeddings based on mask characteristics, balancing background fidelity with generative flexibility. Extensive experiments demonstrate that our approach significantly outperforms existing methods in both visual quality and temporal consistency.

1. Introduction

Video object removal (Kim et al., 2019; Li et al., 2020; Zou et al., 2021; Zhang et al., 2022; Zhou et al., 2023b; Ju et al., 2024; Li et al., 2025b) aims to erase specific objects

¹MT Lab, Meitu Inc., Beijing 100083, China ²Beijing Jiaotong University, Beijing 100044, China. Correspondence to: Ting Liu <lt@meitu.com>.

Proceedings of the 43rd International Conference on Machine Learning, Seoul, South Korea. PMLR 306, 2026. Copyright 2026 by the author(s).

from a video sequence while plausibly synthesizing the missing regions based on the surrounding context. The core challenge lies in reconstructing occluded areas in a manner that ensures spatial coherence within individual frames and temporal consistency across the entire sequence.

Prior works on this task have generally followed two primary directions: propagation-based methods (Kim et al., 2019; Li et al., 2020; Zou et al., 2021; Zhou et al., 2023b; Zhang et al., 2022) and generative inpainting methods (Ju et al., 2024; Li et al., 2025b; Miao et al., 2025). Propagation-based techniques typically rely on optical flow to transfer pixels from non-occluded frames to fill the missing regions. While effective for static scenes, these methods often struggle in complex scenarios involving dynamic camera movements or prolonged occlusions where valid source pixels are unavailable. Conversely, generative approaches formulate object removal as a synthesis problem. The recent emergence of large-scale diffusion models (Podell et al., 2023; Esser et al., 2024; Labs, 2024; Li et al., 2025b) has significantly advanced this domain, enabling the generation of high-fidelity textures and complex structures that were previously unattainable with traditional methods.

Despite these advancements, state-of-the-art video inpainting methods (Li et al., 2025b; Jiang et al., 2025; Miao et al., 2025), particularly those based on diffusion models, predominantly operate under a noise-to-data paradigm. In this standard framework, the generation process initiates from uninformative Gaussian noise and is tasked with denoising this stochastic state into a coherent video sequence conditioned on the masked input. We argue that this formulation is suboptimal for object removal task. Initiating generation from pure noise requires the model to synthesize the entire video content from scratch, often leading to leading to incomplete object erasure or the synthesis of implausible content that conflicts with the scene’s physical logic. To address these stability issues, a common strategy involves reference-guided generation, where a specialized image inpainting model processes a keyframe (usually the first frame) that subsequently serves as a guidance signal (Ouyang et al., 2024; Gao et al., 2025). However, this approach introduces significant drawbacks. It increases system complexity by necessitating an auxiliary image edit model and creates a dependency bottleneck where artifacts in the initial frame

propagate through the sequence, potentially conflicting with the natural temporal evolution of the background.

In this work, inspired by recently proposed bridge models (Chen et al., 2021; Liu et al., 2023; Chen et al., 2023), we propose a paradigm shift by reformulating video object removal as a video-to-video translation task. We posit that the input video, even containing the unwanted object, holds a vast amount of valid structural and environmental information that should be leveraged as a strong prior rather than discarded in favor of Gaussian noise. To realize this, we introduce BridgeRemoval, a novel framework based on the stochastic bridge formulation (Tong et al., 2024; Zhou et al., 2023a; Chen et al., 2023). Unlike standard diffusion-based methods that traverse a path from noise to data, our approach constructs a direct stochastic bridge between the source video distribution (the input video containing the object) and the target video distribution (the clean video with the object removed). By compressing videos into continuous latent representations via a Variational Autoencoder (VAE), we establish a tractable SDE-based generation process where the input latent representation serves directly as the prior boundary distribution.

This bridge formulation anchors the generative trajectory to the source video, naturally enforcing strong spatio-temporal coherence. The model learns a transformation that selectively modifies the object region while preserving the integrity of the unmasked context. Nevertheless, a direct application of this strong prior presents a trade-off. While excellent for background preservation, an overly rigid adherence to the source video can hinder the removal of large objects, as the model may struggle to deviate sufficiently from the input to synthesize large missing regions. To mitigate this, we propose a novel adaptive mask modulation (AMM) strategy. This mechanism dynamically adjusts the influence of the input embeddings based on the spatial characteristics of the mask, allowing the model to relax structural constraints in regions with large occlusions while maintaining strict fidelity in regions with valid backgrounds.

In summary, our contributions are as follows:

- We propose BridgeRemoval, a novel video-to-video generative framework that utilizes an SDE-based bridge model to reformulate video object removal.
- We introduce an adaptive mask modulation strategy that dynamically balances the trade-off between background fidelity and generative flexibility, ensuring robust performance across objects of varying scales.
- Extensive experiments demonstrate the effectiveness of our approach in diverse real-world scenarios, outperforming existing methods in both visual quality and temporal coherence, while also highlighting the

potential of our framework to be extended to other video-to-video edit tasks.

2. Related Works

Diffusion-based Video Object Removal Diffusion-based methods (Li et al., 2025b; Zi et al., 2025; Miao et al., 2025; Jiang et al., 2025; Lee et al., 2025) have achieved state-of-the-art performance in video object removal. DiffuEraser (Li et al., 2025b) adapts the image inpainting architecture of BrushNet (Ju et al., 2024) to the video domain via a progressive two-stage training strategy involving prior propagation and temporal refinement. Beyond simple occlusion handling, ROSE (Miao et al., 2025) addresses complex environmental interactions by leveraging a synthetic dataset with comprehensive supervision to simultaneously remove objects and their collateral visual effects, such as shadows and reflections. Furthermore, unified editing frameworks have also shown promise in this area. VACE (Jiang et al., 2025) proposes a universal backbone for diverse visual conditions, while GenOmnimatte (Lee et al., 2025) employs layered video decomposition, both of which support object removal as a downstream application.

Bridge Models Recently, bridge models (Chen et al., 2021; Tong et al., 2024; Liu et al., 2023; Zhou et al., 2023a; Chen et al., 2023; Zheng et al., 2024; He et al., 2024; De Bortoli et al., 2021; Peluchetti, 2023) have garnered significant attention for their ability to transcend the limitations of the Gaussian prior inherent in standard diffusion models. By establishing a direct stochastic path between two arbitrary distributions, bridge models have demonstrated the clear superiority of a data-to-data generation paradigm over traditional noise-to-data approaches, particularly in tasks such as image-to-image translation (Liu et al., 2023; Zhou et al., 2023a) and speech synthesis (Chen et al., 2023; Li et al., 2025a). Notably, FrameBridge (Wang et al., 2025) successfully extended this methodology to image-to-video (I2V) synthesis by introducing SNR-aligned fine-tuning to stabilize the learning process.

3. Preliminaries

Probability path modeling (De Bortoli et al., 2021; Lipman et al., 2022; Liu et al., 2022) defines a class of generative models that describe continuous-time processes transporting mass from a prior distribution p_1 (source) to a target distribution p_0 (target). Generally, these models are represented by a stochastic differential equation (SDE) (Song et al., 2021):

$$dX_t = v(X_t, t) dt + g(t) dW_t, \quad t \in [0, 1], \quad (1)$$

where $v(X_t, t)$ is the velocity field driving the deterministic trajectory, $g(t)$ controls the stochastic diffusion, and W_t is a standard Brownian motion.

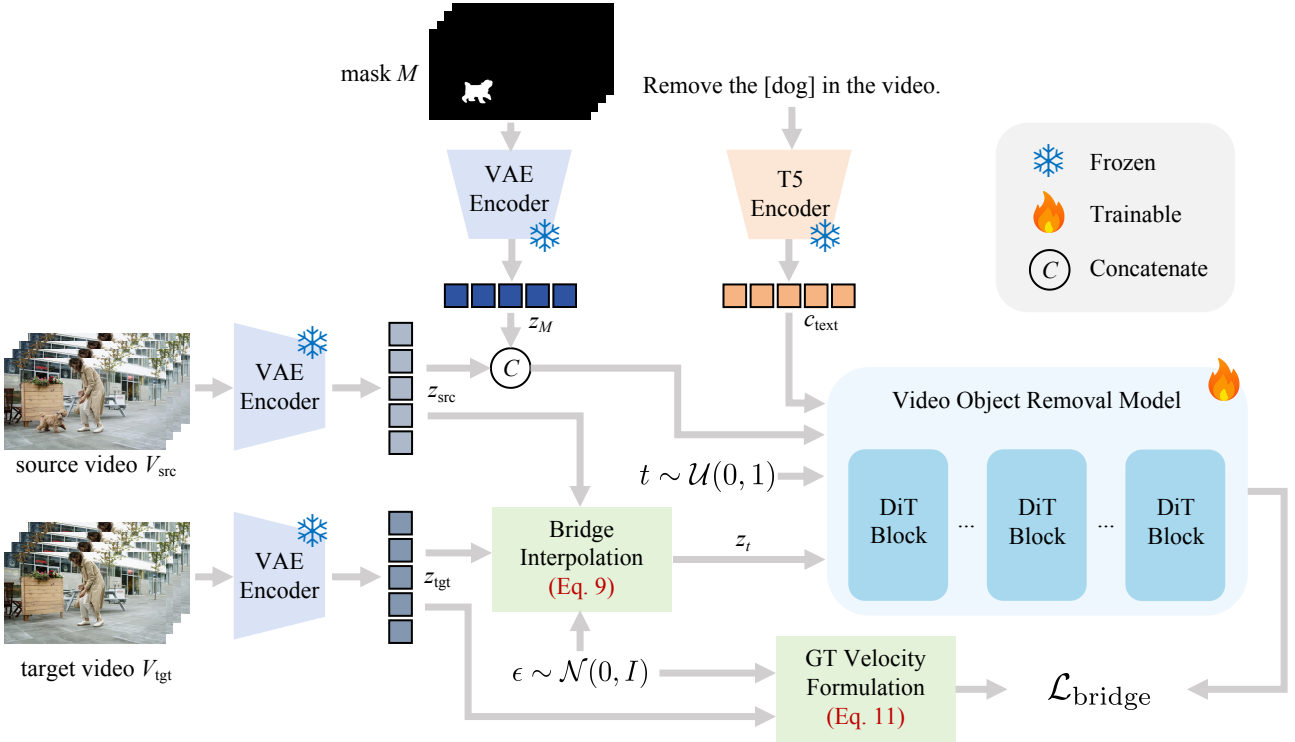


Figure 1. The framework of BridgeRemoval. The video inputs are projected into latent space using a frozen VAE. Unlike standard diffusion, we employ a VP-SDE Bridge formulation to interpolate a trajectory (z_t) directly from the source video prior (z_{src}) to the clean target (z_{tgt}). The DiT-based model is conditioned on text embeddings (c_{text}) and a spatial input formed by concatenating the mask (z_M) with the source latent (z_{src}), optimized via a velocity-matching objective ($\mathcal{L}_{\text{bridge}}$).

3.1. Brownian Bridge

The standard Brownian Bridge (Albergo et al., 2023; Li et al., 2023) is a stochastic process conditioned to start at a specific point x_1 and end at x_0 within a fixed time interval. Unlike standard diffusion which maps data to Gaussian noise, a Brownian Bridge interpolates between two data points. Typically assuming a constant diffusion coefficient, the intermediate state X_t at time t can be written as a linear interpolation perturbed by noise with a fixed variance structure:

$$X_t = (1 - t)x_0 + tx_1 + \sqrt{t(1 - t)}\epsilon, \quad \epsilon \sim \mathcal{N}(0, I). \quad (2)$$

Here, the variance term $t(1 - t)$ is symmetric and reaches its maximum at $t = 0.5$. While simple, this rigid variance schedule limits the model's ability to handle complex transitions where the signal-to-noise ratio needs to be carefully controlled across time.

3.2. VP-SDE Bridge

To enable flexible control over the transport process, we adopt a Variance-Preserving (VP) formulation inspired by the VP-SDE typically used in score-based generative models (Song et al., 2021). We generalize the interpolation

by introducing time-dependent coefficients derived from a noise schedule $\beta(t) \in [\beta_{\min}, \beta_{\max}]$.

Given fixed endpoints x_0 (target) and x_1 (source), the intermediate state X_t is defined by a weighted ternary interpolation:

$$X_t = a_t x_0 + b_t x_1 + c_t \epsilon, \quad \epsilon \sim \mathcal{N}(0, I). \quad (3)$$

The coefficients a_t, b_t, c_t are determined by the variance schedule σ_t :

$$a_t = \frac{\bar{\sigma}_t^2}{\sigma_1^2}, \quad b_t = \frac{\sigma_t^2}{\sigma_1^2}, \quad c_t = \frac{\bar{\sigma}_t \sigma_t}{\sigma_1}, \quad (4)$$

where σ_t^2 represents the cumulative variance at time t , σ_1^2 is the total variance at $t = 1$, and $\bar{\sigma}_t^2 = \sigma_1^2 - \sigma_t^2$. This formulation guarantees boundary conditions satisfying $X_0 = x_0$ and $X_1 = x_1$. By adjusting $\beta(t)$, the VP-SDE Bridge provides a tunable trajectory that is well-suited for high-dimensional video generation tasks.

4. Methodology

As shown in Figure 1, we propose BridgeRemoval, a novel framework for video object removal. Unlike standard diffusion models that generate content from a generic Gaussian

prior, our method leverages the VP-SDE Bridge formulation to construct a direct probability path from the source video (with objects) to the target video (object removed). This approach ensures higher fidelity and better preservation of non-masked regions.

4.1. Latent Encoding and Dual-Role Conditioning

Given a training triplet consisting of a source video V_{src} , a target video V_{tgt} , and a binary mask M , we first project the visual data into a compressed latent space using a pre-trained VAE encoder \mathcal{E} :

$$z_{\text{src}} = \mathcal{E}(V_{\text{src}}), \quad z_{\text{tgt}} = \mathcal{E}(V_{\text{tgt}}), \quad z_M = \mathcal{E}(M). \quad (5)$$

Simultaneously, the text prompt P is encoded into embeddings c_{text} via a T5 encoder.

To provide precise spatial guidance for inpainting, we construct a conditional input y by concatenating the encoded mask with the source latent:

$$y = \text{Concat}(z_M, z_{\text{src}}). \quad (6)$$

It is crucial to note that z_{src} plays a dual role in our framework. First, it acts as the *prior distribution* (the starting point of the bridge at $t = 1$). Second, it serves as a *spatial condition* in y , providing the network with contextual information about the background that should be preserved. This dual utilization effectively anchors the generation process, ensuring seamless blending between the inpainted region and the original background.

4.2. Velocity-Driven Bridge Training

To learn the transition trajectory between the source and target distributions, we frame the video removal task as a stochastic process governed by a Variance-Preserving Stochastic Differential Equation (VP-SDE) (Song et al., 2021).

Bridge Process. Standard diffusion models typically assume an uninformative Gaussian prior $\mathcal{N}(0, I)$. However, our task provides the source video z_{src} as a strong structural prior. To leverage this, we adopt the Bridge Process formulation (Zhou et al., 2023a), replacing the Gaussian prior with a Dirac prior $\delta_{z_{\text{src}}}$.

Specifically, the forward process is modified from the standard diffusion SDE by introducing an additional drift term. The forward SDE is defined as:

$$\begin{aligned} dz_t &= [f(t)z_t + g(t)^2 h(z_t, t, z_{\text{src}})] dt \\ &\quad + g(t)dw, \quad z_0 \sim p_{\text{data}}, \quad z_T = z_{\text{src}}, \end{aligned} \quad (7)$$

where $f(t)$ and $g(t)$ are drift and diffusion coefficients, and $h(z_t, t, z_{\text{src}}) \triangleq \nabla_{z_t} \log p(z_{\text{src}}|z_t)$ acts as a guidance term pulling the trajectory towards z_{src} .

Correspondingly, this process has a reverse process sharing the same marginal distribution, represented by the backward SDE:

$$\begin{aligned} dz_t &= [f(t)z_t - g(t)^2(s_{\theta}(z_t, t, z_{\text{src}}) \\ &\quad - h(z_t, t, z_{\text{src}}))] dt + g(t)d\bar{w}, \end{aligned} \quad (8)$$

where $s_{\theta}(z_t, t, z_{\text{src}}) \triangleq \nabla_{z_t} \log p_{t,\text{bridge}}(z_t|z_{\text{src}})$ approximates the score function. Crucially, since the transition kernel remains Gaussian, the term h is analytically tractable. The learning objective thus reduces to estimating the unknown score term s_{θ} via neural networks.

Training Objective. Instead of simulating the stochastic paths directly via SDE solvers during training, we leverage the property that the marginal distribution of the VP-SDE Bridge at any time t can be derived analytically. This allows us to train the model using a robust velocity-matching objective.

We sample a continuous timestep $t \in [0, 1]$ and a noise variable $\epsilon \sim \mathcal{N}(0, I)$. The intermediate state z_t , following the marginal distribution of Eq. 7, is defined via a ternary interpolation:

$$z_t = a_t z_{\text{tgt}} + b_t z_{\text{src}} + c_t \epsilon. \quad (9)$$

Here, z_t is a weighted mixture of the clean target z_{tgt} , the source prior z_{src} , and the noise ϵ . The scalar coefficients a_t, b_t, c_t are rigorously derived from the variance schedule σ_t of the VP-SDE. Let σ_1 denote the total standard deviation at $t = 1$, and $\bar{\sigma}_t = \sqrt{\sigma_1^2 - \sigma_t^2}$. The coefficients are computed as:

$$a_t = \frac{\bar{\sigma}_t^2}{\sigma_1^2}, \quad b_t = \frac{\sigma_t^2}{\sigma_1^2}, \quad c_t = \frac{\bar{\sigma}_t \sigma_t}{\sigma_1}. \quad (10)$$

These coefficients ensure boundary conditions where $z_0 = z_{\text{tgt}}$ and $z_1 = z_{\text{src}}$.

To train the network v_{θ} parameterized by θ , we define a ground-truth velocity target u_t , derived from the time-derivative of the bridge process (see Appendix):

$$u_t = \frac{a_t}{\rho_t} \epsilon - \frac{c_t}{\rho_t} z_{\text{tgt}}, \quad \text{where } \rho_t = \sqrt{a_t^2 + c_t^2}. \quad (11)$$

The network is optimized by minimizing the mean squared error:

$$\mathcal{L}_{\text{bridge}} = \mathbb{E}_{t, \epsilon, z_{\text{src}}, z_{\text{tgt}}} [\|v_{\theta}(z_t, t, y, c_{\text{text}}) - u_t\|^2]. \quad (12)$$

The complete training procedure is detailed in Algorithm 1.

4.3. Generative Inference via SDE Solver

During inference, we aim to reverse the bridge process to traverse from the source latent z_{src} back to the clean target

Algorithm 1 Training

Input: source video V_{src} , target video V_{tgt} , mask M , text prompt P , VAE encoder \mathcal{E} , T5 encoder, model v_θ , variance schedule σ_t

```

1 repeat
2   Encode latents  $z_{\text{src}} \leftarrow \mathcal{E}(V_{\text{src}})$ ,  $z_{\text{tgt}} \leftarrow \mathcal{E}(V_{\text{tgt}})$ , and  $z_M \leftarrow \mathcal{E}(M)$ 
3   Encode text embeddings  $c_{\text{text}} \leftarrow \text{T5}(P)$ 
4   Construct conditional input  $y \leftarrow \text{Concat}(z_M, z_{\text{src}})$ 
5   Sample interpolation time  $t \sim \mathcal{U}(0, 1)$  and noise  $\epsilon \sim \mathcal{N}(0, I)$ 
6   Compute SDE coefficients  $a_t, b_t, c_t$  based on the variance schedule  $\sigma_t$ 
7   Construct intermediate bridge state  $z_t = a_t z_{\text{tgt}} + b_t z_{\text{src}} + c_t \epsilon$ 
8   Compute normalization factor  $\rho_t = \sqrt{a_t^2 + c_t^2}$ 
9   Compute velocity target  $u_t = \frac{a_t}{\rho_t} \epsilon - \frac{c_t}{\rho_t} z_{\text{tgt}}$ 
10  Update parameters  $\theta$  by gradient descent on  $\|v_\theta(z_t, t, y, c_{\text{text}}) - u_t\|^2$ 
11 until convergence;

```

z_{tgt} . Theoretically, this corresponds to solving the backward SDE (Eq. 8) derived in Sec. 4.2.

Since the continuous backward SDE involves the unknown score function s_θ , we employ a numerical SDE solver to approximate the trajectory. We adopt a variance-corrected sampling strategy that acts as a discretization of the backward SDE, ensuring the generation strictly follows the statistics of the Brownian bridge.

Given the current state z_t at timestep t , the network predicts the velocity field $\hat{v}_t = v_\theta(z_t, t, y)$, which approximates the drift term of the reverse process. We first estimate the clean target latent $\hat{z}_{0|t}$ by inverting the velocity equation (Eq. 11):

$$\hat{z}_{0|t} = \frac{1}{\rho_t^2/c_t} \left(\frac{a_t}{c_t} z_t - \frac{a_t b_t}{c_t} z_{\text{src}} - \hat{v}_t \right). \quad (13)$$

This formula explicitly removes the predicted noise and the weighted source component from z_t , recovering an approximation of the target z_{tgt} .

To progress to the next timestep $t' < t$, we perform a solver step that interpolates between the current state z_t and the predicted target $\hat{z}_{0|t}$, while injecting a calibrated amount of noise ϵ' :

$$z_{t'} = w_1 z_t + w_2 \hat{z}_{0|t} + w_3 \epsilon', \quad \text{with } \epsilon' \sim \mathcal{N}(0, I). \quad (14)$$

Here, w_1, w_2, w_3 are scalar weights analytically determined by the VP-SDE schedule to ensure the trajectory maintains the correct conditional variance. Specifically, w_3 modulates the contribution of the freshly sampled noise ϵ' to prevent variance collapse near the target. The detailed inference algorithm is summarized in Algorithm 2.

Algorithm 2 Inference

Input: source video V_{src} , mask M , text prompt P , trained model v_θ , steps N , variance schedule σ_t , T5 encoder, VAE encoder \mathcal{E} , VAE decoder \mathcal{D}

```

1 Encode input latents  $z_{\text{src}} \leftarrow \mathcal{E}(V_{\text{src}})$  and condition  $y \leftarrow \text{Concat}(\mathcal{E}(M), z_{\text{src}})$ 
2 Encode text embeddings  $c_{\text{text}} \leftarrow \text{T5}(P)$ 
3 Initialize state  $z \leftarrow z_{\text{src}}$  using the source video as the prior
4 Define time schedule  $\{t_k\}_{k=N}^0$  from 1 to 0 for  $k = N, \dots, 1$  do
5   Set current time  $t \leftarrow t_k$  and next time  $t' \leftarrow t_{k-1}$ 
6   Predict velocity field  $\hat{v}_t \leftarrow v_\theta(z, t, y, c_{\text{text}})$ 
7   Recover predicted target  $\hat{z}_{0|t}$  via Eq. 13
8   if  $k > 1$  then
9     Compute SDE solver weights  $w_1, w_2, w_3$  based on  $\sigma_t$ 
10    Sample noise  $\epsilon' \sim \mathcal{N}(0, I)$ 
11    Update state  $z \leftarrow w_1 z + w_2 \hat{z}_{0|t} + w_3 \epsilon'$ 
12  else
13    Set final state  $z \leftarrow \hat{z}_{0|t}$ 
14  end
15 end
16 Decode output video  $V_{\text{out}} \leftarrow \mathcal{D}(z)$ 
Output: Inpainted video  $V_{\text{out}}$ 

```

4.4. Adaptive Mask Modulation

While the bridge formulation effectively anchors the generation trajectory to the source video, thereby ensuring superior background consistency, it introduces a critical trade-off. The source video acts as a strong prior, providing structural guidance that is beneficial for stability. However, this rigid adherence to the source distribution can become detrimental when removing large objects. In such cases, the strong structural prior from the source latent z_{src} may overshadow the generative process, causing the model to struggle in deviating sufficiently from the original content to hallucinate plausible backgrounds for extensive occluded regions.

To mitigate this limitation without sacrificing the benefits of the bridge prior, we propose adaptive mask modulation. This mechanism is designed to dynamically recalibrate the feature influence based on the mask, enhancing the utilization of valid background context while relaxing the constraints on the inpainting region.

Let $h \in \mathbb{R}^{N \times D}$ denote the input patch embeddings to the Transformer, and $M \in \{0, 1\}^{N \times 1}$ be the corresponding binary mask (where 1 denotes the object region and 0 the background). We introduce a learnable modulation parameter γ , initialized to zero. The modulated embeddings h' are computed as:

$$h' = h \odot (M + (1 - M) \cdot (1 + \gamma)). \quad (15)$$

This operation differentially scales the input features:

- Object Region ($M = 1$): Features remain unchanged ($h' = h$), preserving the necessary noise information for the bridge process.
- Background Region ($M = 0$): Features are amplified by a factor of $(1 + \gamma)$.

By adaptively boosting the magnitude of embeddings in the unmasked background regions, AMM effectively increases the “signal-to-noise” ratio of the valid context. In the self-attention mechanism, this amplification acts as a soft bias, encouraging the model to attend more heavily to the reliable background information when synthesizing the missing content. This strategy effectively counterbalances the strong source prior within the masked regions, providing the necessary generative flexibility to reconstruct large occlusions while maintaining strict fidelity to the surrounding environment.

5. Experiments

5.1. Experimental Setup

Training Data. To ensure both geometric precision and semantic diversity, we construct a training dataset totaling approximately 47,000 video pairs from two complementary sources. First, we utilize the ROSE dataset (Miao et al., 2025), which consists of 16,000 synthetically generated samples. By leveraging 3D engines to toggle object visibility, ROSE provides perfectly aligned triplets of source videos, target backgrounds, and masks. While this offers high-quality supervision, our statistical analysis indicates a distribution bias towards static, rigid objects (e.g., signs, furniture), limiting the model’s generalization to complex motion. To address this limitation, we introduce a supplementary real-world composite dataset comprising 31,000 video pairs. This subset is explicitly designed to improve robustness on dynamic agents, containing 15,000 human-centric videos and 16,000 videos of common dynamic objects (e.g., animals, vehicles). The data pipeline adopts a composition-based approach: we employ SAM2 (Ravi et al., 2024) to extract high-fidelity foregrounds from real-world videos and composite them onto clean backgrounds. A Qwen3-VL (Bai et al., 2025) based filtering mechanism is then applied to ensure visual coherence and discard low-quality samples.

Implementation Details. Our model is initialized from the pre-trained Wan2.1-1.3B (Wan et al., 2025). During training, we utilize video clips consisting of 81 frames. To accommodate varying aspect ratios, we employ a bucket-based multi-resolution strategy, where videos are resized to resolutions such as 576×1024 , 1024×576 , or 768×768

based on their original orientation. The bridge process is parameterized with 1000 discrete timesteps during training, utilizing a linear variance schedule with $\beta_{\min} = 0.01$ and $\beta_{\max} = 50.0$. We employ the AdamW optimizer with a constant learning rate of 2×10^{-5} and train the model for 20,000 steps on 8 NVIDIA H100 GPUs. For inference, we use a fast sampling strategy with 50 steps to ensure efficient generation.

Qualitative Comparison. Figures 2, 3, and 4, present a qualitative comparison with GenOmnimatte (Lee et al., 2025), ROSE (Miao et al., 2025), and VACE (Jiang et al., 2025). As shown in the results, our model generates backgrounds with high fidelity and maintains consistent temporal coherence across frames. A notable observation is our model’s behavior in handling unmasked regions: it demonstrates the capacity to implicitly remove associated shadows even when they are not included in the input masks. While baseline methods generally rely on precise masks to define the removal area, our approach appears to leverage a broader context, enabling the seamless erasure of both the target object and its accompanying visual traces.

6. Conclusion

We have presented BridgeRemoval, a stochastic bridge framework that reformulates video object removal as a video-to-video translation task. By leveraging structural priors from the input video and employing an adaptive mask modulation strategy, our method effectively balances background fidelity with generative flexibility. Extensive experiments demonstrate that our approach outperforms existing methods in visual quality and temporal consistency, particularly in handling unmasked artifacts like shadows. This work validates the efficacy of bridge-based models for high-fidelity video inpainting and offers a robust baseline for future video editing research.

Impact Statement

This paper introduces BridgeRemoval, a Bridge-based framework advancing high-fidelity video object removal. While enhancing content creation and post-production, this technology poses potential risks for manipulating authentic footage or altering context. We emphasize the importance of responsible deployment and detection methods to mitigate the misuse of generative video editing tools.

References

Albergo, M. S., Boffi, N. M., and Vanden-Eijnden, E. Stochastic interpolants: A unifying framework for flows and diffusions. *arXiv preprint arXiv:2303.08797*, 2023.

Bai, S., Cai, Y., Chen, R., Chen, K., Chen, X., Cheng, Z.,



Figure 2. Texture quality comparison with the state-of-the-art methods.

Deng, L., Ding, W., Gao, C., Ge, C., Ge, W., Guo, Z., Huang, Q., Huang, J., Huang, F., Hui, B., Jiang, S., Li, Z., Li, M., Li, M., Li, K., Lin, Z., Lin, J., Liu, X., Liu, J., Liu, C., Liu, Y., Liu, D., Liu, S., Lu, D., Luo, R., Lv, C., Men, R., Meng, L., Ren, X., Ren, X., Song, S., Sun, Y., Tang, J., Tu, J., Wan, J., Wang, P., Wang, P., Wang, Q., Wang, Y., Xie, T., Xu, Y., Xu, H., Xu, J., Yang, Z., Yang, M., Yang, J., Yang, A., Yu, B., Zhang, F., Zhang, H., Zhang, X., Zheng, B., Zhong, H., Zhou, J., Zhou, F., Zhou, J., Zhu, Y., and Zhu, K. Qwen3-vl technical report, 2025. URL <https://arxiv.org/abs/2511.21631>.

Chen, T., Liu, G.-H., and Theodorou, E. Likelihood training of schrödinger bridge using forward-backward sdes theory. In *ICLR*, 2021.

Chen, Z., He, G., Zheng, K., Tan, X., and Zhu, J. Schrödinger bridges beat diffusion models on text-to-speech synthesis. *arXiv preprint arXiv:2312.03491*, 2023.

De Bortoli, V., Thornton, J., Heng, J., and Doucet, A. Diffusion schrödinger bridge with applications to score-based generative modeling. In *NeurIPS*, 2021.

Esser, P., Kulal, S., Blattmann, A., Entezari, R., Müller, J., Saini, H., Levi, Y., Lorenz, D., Sauer, A., Boesel, F., et al. Scaling rectified flow transformers for high-resolution image synthesis. In *ICML*, 2024.

Gao, C., Ding, L., Cai, X., Huang, Z., Wang, Z., and Xue, T. Lora-edit: Controllable first-frame-guided video

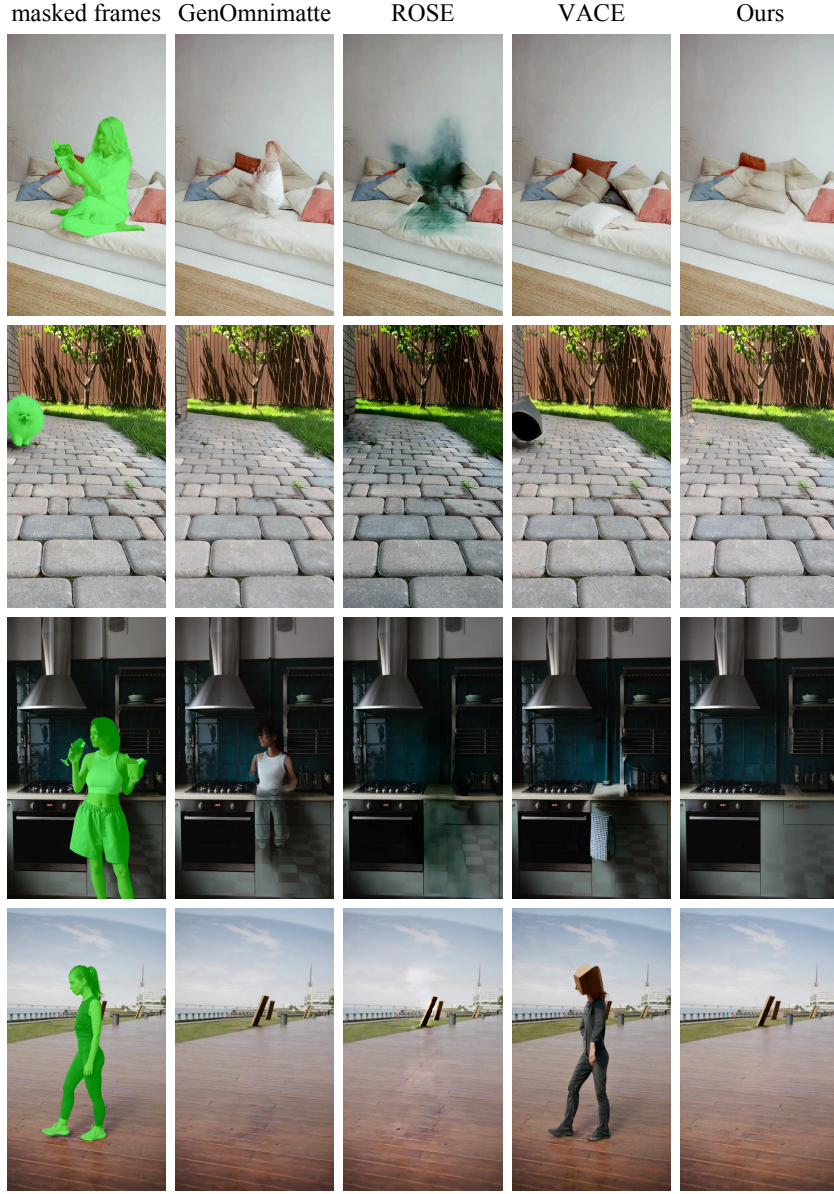


Figure 3. Texture quality comparison with the state-of-the-art methods.

editing via mask-aware lora fine-tuning. *arXiv preprint arXiv:2506.10082*, 2025.

He, G., Zheng, K., Chen, J., Bao, F., and Zhu, J. Consistency diffusion bridge models. In *NeurIPS*, 2024.

Jiang, Z., Han, Z., Mao, C., Zhang, J., Pan, Y., and Liu, Y. Vace: All-in-one video creation and editing. In *ICCV*, 2025.

Ju, X., Liu, X., Wang, X., Bian, Y., Shan, Y., and Xu, Q. Brushnet: A plug-and-play image inpainting model with decomposed dual-branch diffusion. In *ECCV*, 2024.

Kim, D., Woo, S., Lee, J.-Y., and Kweon, I. S. Deep video inpainting. In *CVPR*, 2019.

Labs, B. F. Flux. <https://github.com/black-forest-labs/flux>, 2024.

Lee, Y.-C., Lu, E., Rumbley, S., Geyer, M., Huang, J.-B., Dekel, T., and Cole, F. Generative omnimatte: Learning to decompose video into layers. In *CVPR*, 2025.

Li, A., Zhao, S., Ma, X., Gong, M., Qi, J., Zhang, R., Tao, D., and Kotagiri, R. Short-term and long-term context aggregation network for video inpainting. In *ECCV*, 2020.

Li, B., Xue, K., Liu, B., and Lai, Y.-K. Bbdm: Image-to-

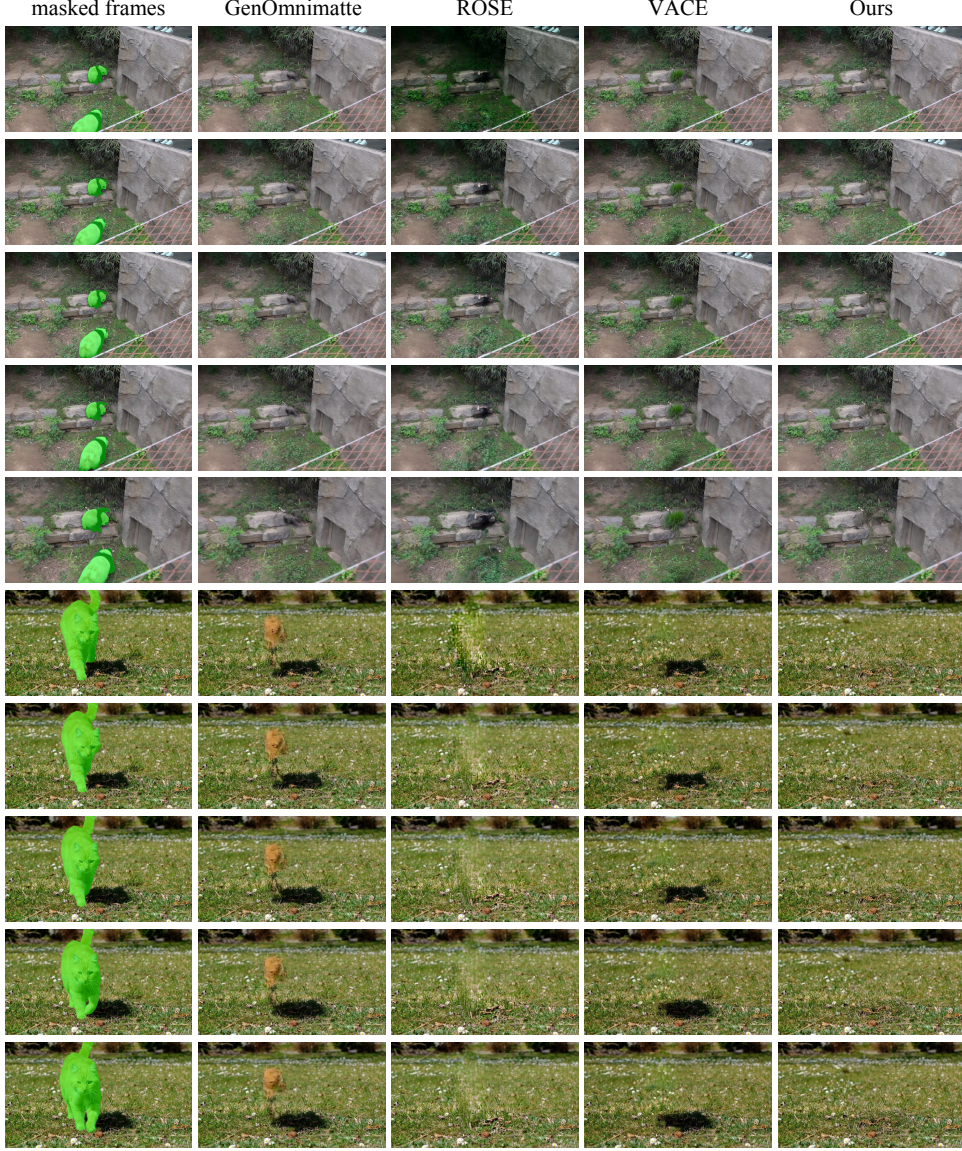


Figure 4. Temporal consistency comparison with the state-of-the-art methods.

image translation with brownian bridge diffusion models. In *CVPR*, 2023.

Li, C., Chen, Z., Bao, F., and Zhu, J. Bridge-sr: Schrödinger bridge for efficient sr. In *ICASSP*, 2025a.

Li, X., Xue, H., Ren, P., and Bo, L. Diffueraser: A diffusion model for video inpainting. *arXiv preprint arXiv:2501.10018*, 2025b.

Lipman, Y., Chen, R. T., Ben-Hamu, H., Nickel, M., and Le, M. Flow matching for generative modeling. *arXiv preprint arXiv:2210.02747*, 2022.

Liu, G.-H., Vahdat, A., Huang, D.-A., Theodorou, E. A.,

Nie, W., and Anandkumar, A. I^2 sb: Image-to-image schrödinger bridge. In *ICML*, 2023.

Liu, X., Gong, C., and Liu, Q. Flow straight and fast: Learning to generate and transfer data with rectified flow. *arXiv preprint arXiv:2209.03003*, 2022.

Miao, C., Feng, Y., Zeng, J., Gao, Z., Liu, H., Yan, Y., Qi, D., Chen, X., Wang, B., and Zhao, H. Rose: Remove objects with side effects in videos. *arXiv preprint arXiv:2508.18633*, 2025.

Ouyang, W., Dong, Y., Yang, L., Si, J., and Pan, X. I2vedit: First-frame-guided video editing via image-to-video diffusion models. In *SIGGRAPH Asia*, 2024.

Peluchetti, S. Non-denoising forward-time diffusions. *arXiv preprint arXiv:2312.14589*, 2023.

Podell, D., English, Z., Lacey, K., Blattmann, A., Dockhorn, T., Müller, J., Penna, J., and Rombach, R. SDXL: Improving latent diffusion models for high-resolution image synthesis. *arXiv preprint arXiv:2307.01952*, 2023.

Ravi, N., Gabeur, V., Hu, Y.-T., Hu, R., Ryali, C., Ma, T., Khedr, H., Rädle, R., Rolland, C., Gustafson, L., et al. Sam 2: Segment anything in images and videos. *arXiv preprint arXiv:2408.00714*, 2024.

Song, Y., Sohl-Dickstein, J., Kingma, D. P., Kumar, A., Ermon, S., and Poole, B. Score-based generative modeling through stochastic differential equations. In *ICLR*, 2021.

Tong, A., Malkin, N., Fatras, K., Atanackovic, L., Zhang, Y., Huguet, G., Wolf, G., and Bengio, Y. Simulation-free schrödinger bridges via score and flow matching. In *ICAIS*, 2024.

Wan, T., Wang, A., Ai, B., Wen, B., Mao, C., Xie, C.-W., Chen, D., Yu, F., Zhao, H., Yang, J., et al. Wan: Open and advanced large-scale video generative models. *arXiv preprint arXiv:2503.20314*, 2025.

Wang, Y., Chen, Z., Chen, X., Wei, Y., Zhu, J., and Chen, J. Framebridge: Improving image-to-video generation with bridge models. In *ICLR*, 2025.

Zhang, K., Fu, J., and Liu, D. Flow-guided transformer for video inpainting. In *ECCV*, 2022.

Zheng, K., He, G., Chen, J., Bao, F., and Zhu, J. Diffusion bridge implicit models. *arXiv preprint arXiv:2405.15885*, 2024.

Zhou, L., Lou, A., Khanna, S., and Ermon, S. Denoising diffusion bridge models. In *ICLR*, 2023a.

Zhou, S., Li, C., Chan, K. C. K., and Loy, C. C. Propainter: Improving propagation and transformer for video inpainting. In *ICCV*, 2023b.

Zi, B., Peng, W., Qi, X., Wang, J., Zhao, S., Xiao, R., and Wong, K.-F. Minimax-remover: Taming bad noise helps video object removal. *arXiv preprint arXiv:2505.24873*, 2025.

Zou, X., Yang, L., Liu, D., and Lee, Y. J. Progressive temporal feature alignment network for video inpainting. In *CVPR*, 2021.